Predicting the tensile strength, impact toughness, and hardness of friction stir welded AA 6061-T6 using response surface methodology

Wasif safeen[1], Salman Hussain[1], Ahmad Wasim[1], Mirza Jahanzaib[1], Haris Aziz[1], Hassan Abdalla[2]
[1]Department of Industrial Engineering, University of Engineering and Technology Taxila, Pakistan
[2]School of Architecture, Computing and Engineering, University of East London, UK

Abstract

In this research an attempt has been made to develop mathematical models for predicting mechanical properties including ultimate tensile strength, impact toughness, and hardness of the friction stir welded AA 6061-T6 joints at 95% confidence level. Response surface methodology with central composite design having four parameters and five levels has been used. The four parameters considered were tool pin profile, rotational speed, welding speed and tool tilt angle. Three confirmation tests were performed to validate the empirical relations. In addition, the influence of the process parameters on ultimate tensile strength, impact toughness, and hardness were investigated. The results indicated that tool pin profile is the most significant parameter in terms of mechanical properties; tool with simple cylindrical pin profile produced weld with high ultimate tensile strength, impact toughness, and hardness. In addition to tool pin profile, rotational speed was more significant compared to welding speed for ultimate tensile strength and impact toughness; whereas, welding speed showed dominancy over rotational speed in case of hardness. Optimum conditions of process parameters have been found at which tensile strength of 92%, impact toughness of 87%, and hardness of 95% was achieved in comparison to the base metal. This research will contribute to expand the scientific foundation of friction stir welding of Aluminum alloys with emphasis on AA 6061-T6. The results will aid the practitioners to develop a clear understanding of the influence of process parameters on mechanical properties, and will allow the selection of best combinations of parameters to achieve desired mechanical properties.

Keywords

Friction stir welding, parameters, response surface methodology, tensile strength, impact toughness, hardness

1. Introduction

The manufacturing industries including automotive, aerospace, shipbuilding, and railway develop products ranging from simple to complex shapes. To enhance the performance of products, these industries are focusing on high strength to weight ratio metals for reducing overall weight of the product without compromising the quality. Copper and Aluminum alloys are the examples of widely applicable high strength to weight ratio metals. In most cases, the manufacturing of complex products using these metals as a single part without joints is technically infeasible. Conventionally, these metals are joined by metal inert gas welding, tungsten inert gas welding, gas tungsten arc welding, and gas metal arc welding. These conventional joining methods cause porosity, high residual stresses, segregation, lack of fusion, shrinkage during solidification, and high solubility of hydrogen and other gases which ultimately reduce strength of the weld [1-7]. Friction Stir Welding (FSW) is a solid state non-conventional joining technique which has the capability to address the above limitations [8-9]. Furthermore, both similar [10-12] and dissimilar [13-15] metals can be joined by FSW. FSW is an environment friendly green process which does not require filler material unlike conventional welding methods. In FSW, a rotating non-consumable tool moves between the joining line of two metals. Due to friction between rotating tool and metal, heat is generated which softens and fuses the metals to form a good quality weld [16]. The weld produced by FSW exhibits better mechanical properties as compared to conventional welding processes [17, 18]. For example, Zhao et al. [19] welded Al–Mg–Sc alloy by FSW and tungsten inert gas welding. The results indicated that tensile strength of FSW was 19% higher than tungsten inert gas welding. Lakshminarayanan et al. [20] also compared the tensile strength of AA6061 weld produced by FSW, gas tungsten arc welding, and gas metal arc welding. The authors demonstrated that tensile strength of friction stir welded parts was 19% and 22% higher than gas tungsten arc welded parts and gas metal arc welded parts respectively.

The quality and strength of friction stir (FS) weld can be evaluated by mechanical properties such as tensile strength, impact toughness and hardness. However, hardness is the critical measure which directly affects tensile strength. This is because the tensile failure occurs along the weakest path in term of hardness [21]. To increase hardness of Aluminum alloys, various researchers have investigated the effects of interlayer, external cooling, post weld heat treatment and tempering [18, 22-24]. The mechanical properties of the FS weld greatly depend on the process parameters including tool pin profile, rotational speed, welding speed, and tool tilt angle [15, 18, 21-37]. A number of researchers have investigated the effect of various process parameters on mechanical properties of FSW. Xu et al. [25] investigated the influence of tool pin profile on FS welded AA2219. The results indicated that tapered threaded tool with flutes pin profile produced weld with good mechanical properties. The effect of tool pin profile on FS welded AA6061 was investigated by Elangovan et al. [26] and reported that tool with square pin profile produced weld with high strength. Palanivel et al. [27] also reported that high tensile strength can be achieved by square tool pin profile while joining two dissimilar AA5083-H111 and AA6351-T6 aluminum alloys by FSW. Salari et al. [28] investigated the effect of tool pin profile on the mechanical properties of FS welded AA5456. The results indicated that tool pin with stepped conical threaded profile produced weld with superior mechanical properties. Ilangovan et al. [29] joined two aluminum alloys AA6061 and AA5086 and examined the effect of tool pin profile on the weld. It was discovered that threaded cylindrical pin produced a sound and defect free weld. Mohanty et al. [30] reported that straight cylindrical pin profile produced good quality weld on FSW of aluminum alloys.

The welding and rotational speeds also affect the properties of the weld. Movahedi et al. [32] identified that defects at the weld nugget can be reduced by decreasing welding speed; contemporarily, weld strength can be increased by decreasing welding speed. Kasman [33] reported that mechanical properties were more sensitive to welding speed than rotational speed in welding of dissimilar Aluminum alloys AA6082-T6 and AA5754-H111. Similarly, Aydin et al. [34] examined that welding speed has the most significant effect on tensile strength of FS welded of AA1050. Jayaraman et al. [35] on the other hand, concluded that rotational speed has the most significant effect on tensile strength of FS welded A319. Ahmadi et al. [38] investigated the effect of rotational speed, welding speed, and tilt angle and reported that tilt angle has the least significant effect on mechanical properties.

Aluminum Alloy 6061-T6 has high strength to weight ratio and good corrosion resistance. Because of its wide application in the field of manufacturing, it is extensively investigated by researchers. Liu et al. [39] investigated the tensile strength of FS welded AA 6061-T6 and reported that tensile strength increases with the increase in welding speed. Li et al. [40] joined two AA 6061-T6 plates by tool with stationary shoulder and concluded that mechanical properties depends on welding speed. Rajakumar et al. [41] developed regression models to predict tensile behavior, hardness and corrosion rate of FS welded AA 6061-T6 using response surface methodology. Fujii et al. [42] discovered that mechanical properties were not dependent on tool pin profile for AA6061-T6.

Various statistical and mathematical tools including regression, Taguchi method, response surface methodology (RSM), simulated annealing and artificial neural network have been used by researchers to model and optimize the friction stir welding process parameters of aluminum alloys [33-35, 43-47]. However, RSM with central composite design has the superior capability to predict and optimize responses due to more number of levels [48]. Elangovan et al. [49] applied RSM to estimate tensile strength of FS welded AA6061 aluminum alloy. Heidarzadeh et al. [50] used RSM to predict the tensile strength of FS welded AA 6061-T4. Lotfi and Nourouzi [51] employed RSM to model tensile behavior and microhardness of the FS welded AA7075-T6. Ilkhichi et al. [52] developed a mathematical model to predict grain size and hardness of FS welded AA 7020 using RSM.

From the literature review, it can be concluded that the researchers have proposed different pin profiles for different materials to produce good quality weld. Some researchers proposed square pin profile while other proposed cylindrical pin profile. Likewise, some researchers reported welding speed as most significant parameter; whereas, other identified rotational speed as an important contributing factor. Similarly, tool tilt angle has been used by previous researchers but it was referred as insignificant parameter. However, the exact behavior of these process parameters on mechanical properties of AA 6061-T6 still need to be investigated. This research presents a systematic approach to quantify the influence of process parameters on mechanical properties. Therefore, the aim of this research is to develop an empirical relationship using RSM to predict the ultimate tensile strength (UTS), impact toughness, and hardness of FS welded AA 6061-T6 and to optimize the process parameters to maximize these mechanical properties. Furthermore, the influence of tool pin profile, rotational speed, welding speed, and tool tilt angle on UTS, impact toughness, and hardness of FS welded AA 6061-T6 has also been investigated.

2. Experimental procedure

This section describes the details regarding the experimental setup, welding conditions, and methodology adopted for the study. Two plates of AA6061-T6 each with dimensions of 120 mm x 100 mm x 5 mm were joined by FSW in this research. The chemical composition and mechanical properties of AA6061-T6 are presented in Table 1. The ultimate tensile strength, impact toughness, and hardness of AA6061-T6 are 312 MPa, 17 J, and 108 HV, respectively. The tools were manufactured from molybdenum based high speed steel due to its good wear resistant property. The chemical composition of the tool material is given in Table 2. Five tools with different pin profiles have been used in this study. These profiles include simple cylindrical (SC), cylindrical with threads (CT), simple tapered (ST), tapered with threads (TT), and simple square (SS) as shown in Figure 1. Each tool had the same dimension of pin diameter of 6 mm, pin length of 4.7 mm, and shoulder diameter of 18 mm with 6° concavity at the bottom side. The pin base and tip diameter for ST and TT was 6 mm and 4 mm respectively; whereas, the plunge depth was 0.1 mm. Conceptual diagram of simple cylindrical tool is given as example in Figure 2. Since during FSW, the tool is subjected to high mechanical and thermal stresses therefore there were high chances of tool damage. To avoid tool damage, tools were heat treated and hardened to 61 HRC. Four welding parameters namely tool pin profile, rotational speed, welding speed, and tool tilt angle have been used in this study. The joints were fabricated using an indigenously design FSW machine with computer numeral control in position control mode. The backing plate used in the experiments was made of cost iron. The entire welds have the same length of 120 mm. After each experiment the work-piece was labeled precisely. For example, a friction stir weld, produced by simple cylindrical tool pin profile with rotational speed of 1150 rpm, welding speed of 70 mm/min, and tilt angle of 3°, is shown in Figure 3.

Table 1: Chemical composition of Aluminum Alloy 6061-T6

Chemical composition									Mechanical properties		
Al	Mn	Si	Fe	Zn	Ti	Cr	Mg	Cu	UTS (MPa)	Impact toughness (J)	Hardness (HV)
Bal	0.03	0.61	0.20	0.02	0.01	0.13	0.81	0.29	312	17	108

Table 2: Chemical composition of tool material

Element	C	Mn	Si	P	S	Ni	Cr	Mo	Cu
%	1.0	0.33	0.30	0.03	0.008	0.16	3.90	5.20	0.14

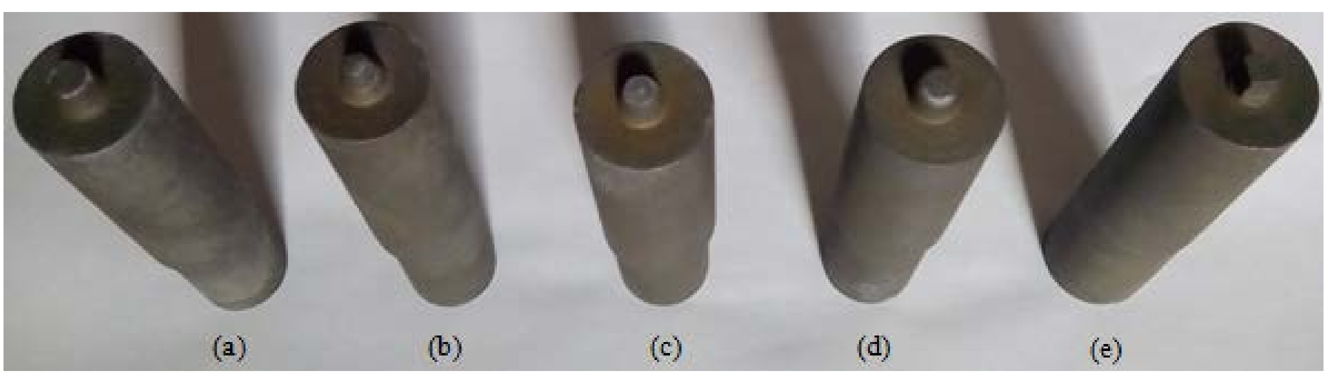

Figure 1. Manufactured tools (a) cylindrical threaded (b) tapered threaded (c) simple tapered (d) simple cylindrical (e) simple square

Figure 2. Conceptual diagram of simple cylindrical tool

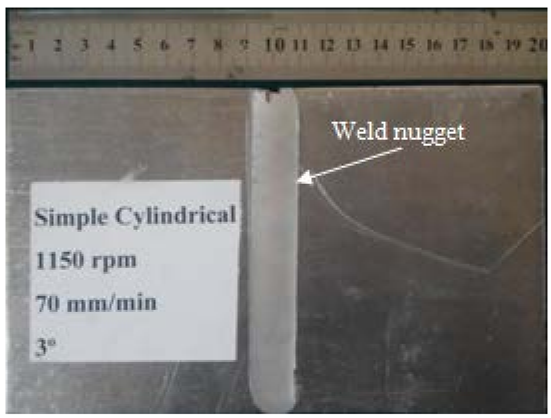

Figure 3. Welded sample

The mechanical properties of the welded joints were evaluated by ultimate tensile strength (UTS), impact toughness, and hardness. The samples for UTS, impact toughness, and hardness were prepared perpendicular to the direction of weld as shown in Figure 4. The UTS of the welded plates was evaluated according to ASTM E8M-04. Three samples from each welded plate were tested and average was calculated to minimize error. The UTS samples were extracted to the required dimensions as shown in Figure 5. The prepared samples were tested on universal testing machine with a capacity of 500 kN. The cross head speed was 1 mm/min during testing. For evaluation of impact toughness of the joints, ASTM E23-04 guidelines were followed. Charpy impact samples were prepared according to the dimensions shown in Figure 6. The impact test was conducted on pendulum type machine (Make: Zwick and Model: HIT50P) with maximum capacity of 50 J. The hardness test was performed on Vickers hardness test machine (Make: Shimadzu and Model: HMV-2T) with 0.05 kg load for 15 seconds. The hardness was measured at the top surface of the weld.

Three readings were taken in total out of which two were taken near the top and bottom edge; whereas, the third one at the middle of the hardness sample. The hardness value was obtained by averaging the three readings. The results are presented in Table 4 along with respective parameters. For example, with tapered threaded pin profile, rotational speed of 1000 rpm, welding speed of 50 mm/min, and tilt angle of 2^{o}, ultimate tensile strength of 249.38 MPa, impact toughness of 10 J, and hardness of 64 HV was achieved. Furthermore, it can be seen that highest UTS of 288.10 MPa, impact toughness of 14.73 J, and hardness of 103 HV has been achieved at rotational speed of 1150 rpm, welding speed of 70 mm/min, tilt angle of 3^{o}, and with simple cylindrical tool. These values are 92% of UTS, 87% of impact toughness, and 95% of hardness as compared to parent material.

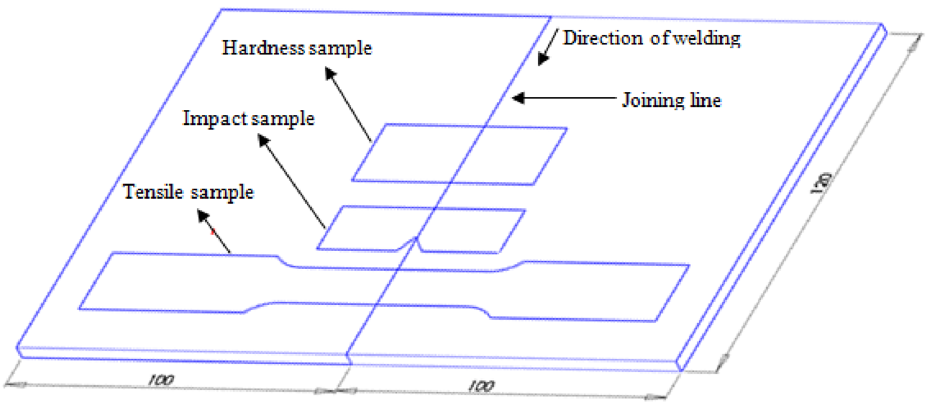

Figure 4. Position of samples

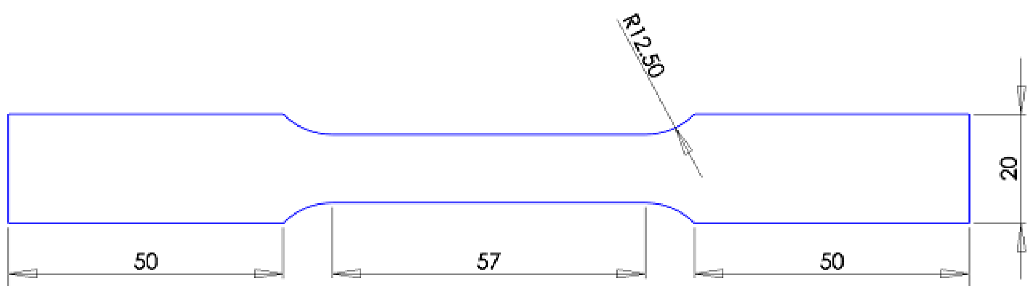

Figure 5. Sample for tensile test

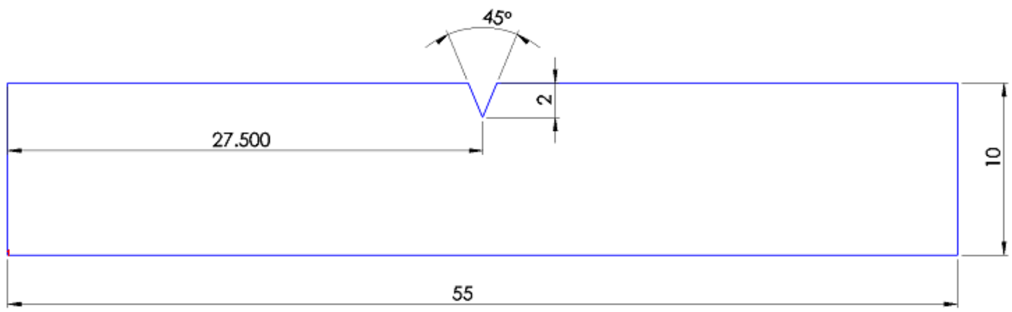

Figure 6. Sample for impact toughness

3. Experimental design

Trial runs were performed before the experimentation to identify the FSW parameters that effects the mechanical properties of friction stir welded AA6061-T6. Based on these runs, the important FSW parameters that are used in the current research are tool pin profile, rotational speed, welding speed, and tool tilt angle. RSM with central composite rotatable design was used in this investigation. Central composite rotatable design requires five levels for each parameter. The upper and lower limits of the parameters were chosen in such a way that the resulting weld is free from defects. The upper limit of the parameters was coded as +2 and the lower limit was coded as -2. The other coded values were calculated using the following equation.

$$X_i=2[2X-(X_{max}+X_{min})]/(X_{max}-X_{min}) \quad (1)$$

where X_i in the above equation is the resulting coded value of a variable X; X is any value of the variable from X_{min} to X_{max}; X_{min} is the lower and X_{max} is the upper limit of the variable. The parameters with levels are shown in Table 3.

Table 3: FSW parameters with levels

Parameters	**Levels**				
	-2	-1	0	+1	+2
Pin profile, P	SS	TT	SC	CT	ST
Rotational speed, N (rpm)	850	1000	1150	1300	1450
Welding speed, S (mm/min)	30	50	70	90	110
Tilt angle, T	1°	2°	3°	4°	5°

Overall 30 experiments with four factors and five levels were performed, as shown in Table 4. These experiments were calculated by the following relation [53]:

No. of experiments = $2^n + 2n + n_c$

(2)

Where n is the number of selected factors and n_c is the number of experiments on center points. The value of n_c varies from 4 to 6. In this research, the numbers of selected factors (n) were 4 and number of experiments on center points (n_c) were 6.

Table 4: Experimental design matrix

Experiment Number	Input parameters				Output responses		
	Rotational Speed (rpm)	Welding Speed (mm/min)	Tilt Angle	Pin Profile	UTS (MPa)	Impact toughness (J)	Hardness (HV)
1	1000	50	2°	TT	249.38	10	64
2	1300	50	2°	TT	211.26	8.6	55
3	1000	90	2°	TT	180.41	9.55	59
4	1000	50	4°	TT	244.49	7.81	61
5	1000	50	2°	CT	258.37	9.24	79
6	1300	90	4°	CT	261.50	9.4	70
7	1000	90	4°	CT	252.07	8.82	74
8	1300	50	4°	CT	253.44	7.6	69
9	1300	90	2°	CT	255.93	11.68	78
10	1300	90	4°	TT	209.59	12	61
11	1000	50	4°	CT	250.46	13.5	68
12	1000	90	2°	CT	255.44	13.31	74
13	1000	90	4°	TT	183.81	9.65	57
14	1300	50	2°	CT	254.28	14.22	81
15	1300	50	4°	TT	187.38	10.8	53
16	1300	90	2°	TT	198.06	9.6	67
17	1450	70	3°	SC	272.99	11.23	81
18	850	70	3°	SC	265.62	10.95	89
19	1150	110	3°	SC	255.00	11.64	97
20	1150	30	3°	SC	286.72	12.99	88
21	1150	70	5°	SC	270.88	13.49	76
22	1150	70	1°	SC	258.18	13.86	83
23	1150	70	3°	ST	154.95	10.85	62
24	1150	70	3°	SS	164.00	9.56	51
25	1150	70	3°	SC	288.10	14.13	98
26	1150	70	3°	SC	286.02	13.98	89
27	1150	70	3°	SC	264.65	13.47	103
28	1150	70	3°	SC	283.92	13.4	95
29	1150	70	3°	SC	253.04	14.73	91

30	1150	70	3°	SC	283.99	14.21	101

4. Results and discussions

4.1 Development of mathematical models

A mathematical model was developed to predict mechanical properties including ultimate tensile strength, impact toughness, and hardness of FS welded AA 6061-T6 at different welding conditions. The ultimate tensile strength (UTS), impact toughness (IT), and hardness (H) of the FS welded joints are function of tool pin profile (P), rotational speed (N), welding speed (S), and tool tilt angle (T). The quadratic regression equation to represent the 3D response surface is given by:

$$Y = b_0 + \sum b_i x_i + \sum b_{ii} x_i^2 + \sum b_{ij} x_i x_j$$

(3)

Where Y is the response, the term b_0 is the mean of responses and the terms b_i, b_{ii}, and b_{ij} are the coefficients of responses and it depends on the respective main and interaction effects of the parameters. x_i and x_j are the coded independent variables.

The values of the coefficients can be calculated by regression analysis with the help of following equations [54]:

$$b_o = 0.142857\Sigma(Y) - 0.035\ 714\Sigma\Sigma(X_{ii} Y)$$

(4)

$$b_i = 0.041667\Sigma(X_i Y)$$

(5)

$$b_{ii} = 0.03125\Sigma(X_{ii} Y) + 0.003\ 72\Sigma\Sigma(X_{ii} Y) - 0.035\ 714\Sigma(Y)$$

(6)

$$b_{ij} = 0.0625\Sigma(X_i Y)$$

(7)

For four factors, the second order polynomial could be expressed as:

UTS (or) IT (or) H =

$b_0+b_1P+b_2N+b_3S+b_4T+b_{11}P^2+b_{22}N^2+b_{33}S^2+b_{44}T^2+b_{12}PN+b_{13}PS+b_{14}PT+b_{23}NS+b_{24}NT+b_{34}ST$
(8)

The coefficients of the regression model for UTS, impact toughness, and hardness were calculated at confidence level of 95% using Design-Expert software (version 9.0). The summary of model statistics indicated that quadratic is best suggested; therefore, it has been used for predicting the responses. The final regression models for UTS, impact toughness, and hardness are given in equation 9, 10 and 11 respectively.

$$\text{Ultimate tensile strength} = 276.62 + 14.96(P) - 1.18(N) - 7.32(S) + 0.21(T) + 3.79(P)(N) + 8.07(P)(S) + 0.46(P)(T) +9.35(N)(S) + 0.32(N)(T) + 3.42(S)(T) - 30.86 (P^2) - 3.40(N^2) - 3.01(S^2) - 4.59(T^2) \quad (9)$$

$$\text{Impact toughness} = 13.99 + 1.08(P) + 0.14(N) - 0.17(S) - 0.33(P)(N) + 0.45(P)(S) - 0.37(N)(S) -0.32(N)(T) + 0.16(S)(T) - 1.46(P^2) - 0.74(N^2) - 0.43(S^2) \quad (10)$$

$$\text{Hardness} = 96.17 + 5.75(P) - 0.75(N) + 1.17(S) - 2.42(T) - 0.75(P)(S) - 1.13(P)(T) + 1.63(N)(S) - 11.83 (P^2) - 4.71(N^2) - 2.83(S^2) - 6.08(T^2) \quad (11)$$

4.2 Adequacy of the models

Adequacy measures the fitness of the proposed model to predict the output response. The adequacy of the developed models was evaluated using Analysis of Variance (ANOVA). The ANOVA results for UTS, impact toughness, and hardness are given in Table 5, 6, and 7, respectively. The results show that all the three models are significant. The model terms for which the p-value is less than 0.05 are significant model terms. In case of UTS, P and P^2 are significant model terms, for impact toughness P, PS, N^2, S^2, D^2 and for hardness P, N^2, T^2, D^2 are significant model terms. Coefficient of determination (R^2) is another creteria used to evaluate the adequacy of a model. For an ideal model, the value of R^2 is unity. For UTS, impact toughness, and hardness the values of R^2 are 0.85, 0.92, and 0.84, respectively. Adequate precision measures the signal to noise ratio and its value more than 4 is desirable. For UTS, impact toughness, and hardness the value of adequate presicion are 10.59, 14.67, and 9.72, repectively, which indicates an adequate signal. In addition to ANOVA, normal plot of residuals and graph of actual vs. predicted values have also been drawn. The normal plot of residuals is used to verify normality assumptions; whereas, the graph of predicted vs. actual values demonstrates the prediction capability of developed model [53]. The normal plot of residuals of the UTS, impact toughness, and hardness are shown in Figure 7(a), 7(b), and 7(c). All points lies on the line which indicates the error is normally distributed. The graph of predicted vs. actual values for UTS, impact toughness, and hardness are shown in Figure 8(a), 8(b), and 8(c). The points lie close to the actual values which show the predicted values are in good agreement with actual values.

Table 5: ANOVA for ultimate tensile strength

Source	Sum of Squares	DF	Mean Square	F-Value	p-value
Model	35748.50	14	2553.46	5.891	0.0008
P	5369.92	1	5369.92	12.389	0.0031
N	33.26	1	33.26	0.077	0.7856
S	1285.98	1	1285.98	2.967	0.1055
T	1.04	1	1.04	0.002	0.9615
PN	229.69	1	229.69	0.530	0.4778
PS	1040.97	1	1040.97	2.402	0.1420
PT	3.34	1	3.34	0.008	0.9312
NS	1399.88	1	1399.88	3.230	0.0925
NT	1.67	1	1.67	0.004	0.9514
ST	186.66	1	186.66	0.431	0.5216
P^2	26115.79	1	26115.79	60.254	0.0001
N^2	317.12	1	317.12	0.732	0.4058
S^2	248.65	1	248.65	0.574	0.4605
T^2	578.68	1	578.68	1.335	0.2660
Residual	6501.40	15	433.43		
Lack of Fit	5474.48	10	547.45	2.665	0.1454
Pure Error	1026.92	5	205.38		
Cor Total	42249.90	29			
Std. Dev.	20.82		R-Squared		0.8461
Mean	243.13		Adj R-Squared		0.7025
C.V. %	8.56		Pred R-Squared		0.2187
PRESS	33011.77		Adeq Precision		10.593

Table 6: ANOVA for impact toughness

Source	Sum of Squares	DF	Mean Square	F-Value	p-value
Model	107.25	14	7.66	12.85	< 0.0001
P	28.04	1	28.03	47.04	< 0.0001
N	0.48	1	0.47	0.79	0.3856
S	0.69	1	0.68	1.15	0.3000
T	0.10	1	0.10	0.17	0.6858

PN	1.79	1	1.79	3.01	0.1031
PS	3.29	1	3.29	5.52	0.0328
PT	0.24	1	0.24	0.40	0.5352
NS	2.19	1	2.19	3.67	0.0745
NT	1.67	1	1.67	2.81	0.1142
ST	0.38	1	0.38	0.64	0.4345
P^2	58.60	1	58.60	98.32	< 0.0001
N^2	15.07	1	15.03	25.22	0.0002
S^2	5.17	1	5.17	8.67	0.0100
T^2	0.24	1	0.24	0.40	0.5326
Residual	8.93	15	0.59		
Lack of Fit	7.70	10	0.77	3.12	0.1104
Pure Error	1.23	5	0.24		
Cor Total	116.19	29			
Std. Dev.	0.77		R-Squared		0.9231
Mean	11.80		Adj R-Squared		0.8512
C.V. %	6.54		Pred R-Squared		0.6027
PRESS	46.16		Adeq Precision		14.670

Table 7: ANOVA for hardness

Source	Sum of Squares	DF	Mean Square	F-Value	p-value
Model	5630.71	14	402.19	5.48	0.0011
P	793.5	1	793.5	10.81	0.0050
N	13.5	1	13.5	0.18	0.6740
S	32.66	1	32.66	0.44	0.5147
T	140.16	1	140.16	1.91	0.1871
PN	4	1	4	0.054	0.8185
PS	9	1	9	0.12	0.7310
PT	20.25	1	20.25	0.27	0.6069
NS	42.25	1	42.25	0.57	0.4596
NT	9	1	9	0.12	0.7310
ST	9	1	9	0.12	0.7310
P^2	3840.76	1	3840.76	52.37	< 0.0001
N^2	608.04	1	608.04	8.29	0.0115
S^2	220.19	1	220.19	3.002	0.1036
T^2	1015.04	1	1015.04	13.84	0.0021
Residual	1100.08	15	73.33		
Lack of Fit	947.25	10	94.72	3.098	0.1118
Pure Error	152.83	5	30.56		
Cor Total	6730.8	29			
Std. Dev.	8.56		R-Squared		0.8366
Mean	75.80		Adj R-Squared		0.6840
C.V. %	11.30		Pred R-Squared		0.1567
PRESS	5676.24		Adeq Precision		9.716

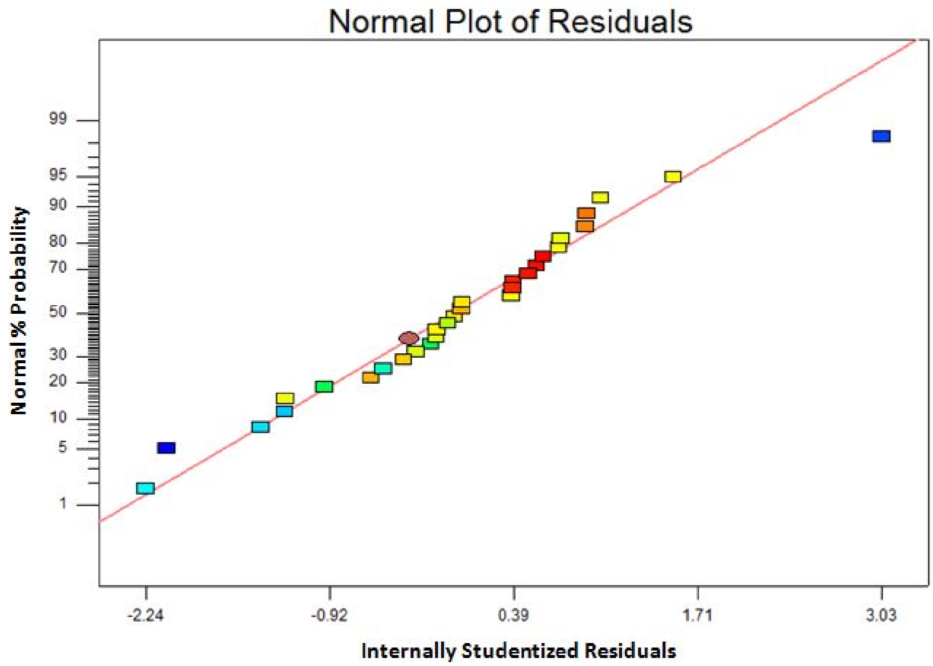

(a) Normal plot of residuals for ultimate tensile strength

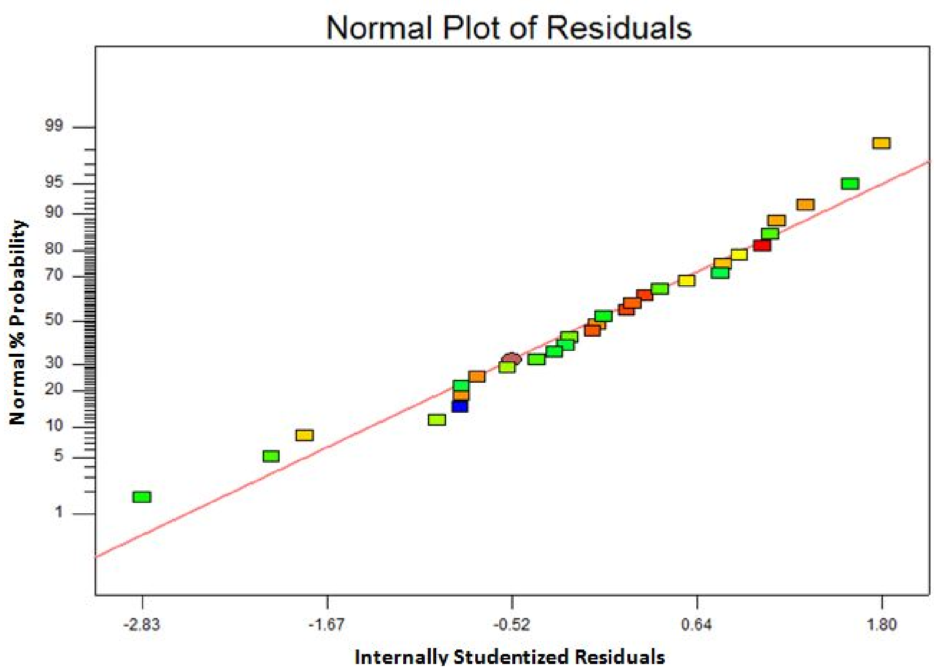

(b) Normal plot of residuals for impact toughness

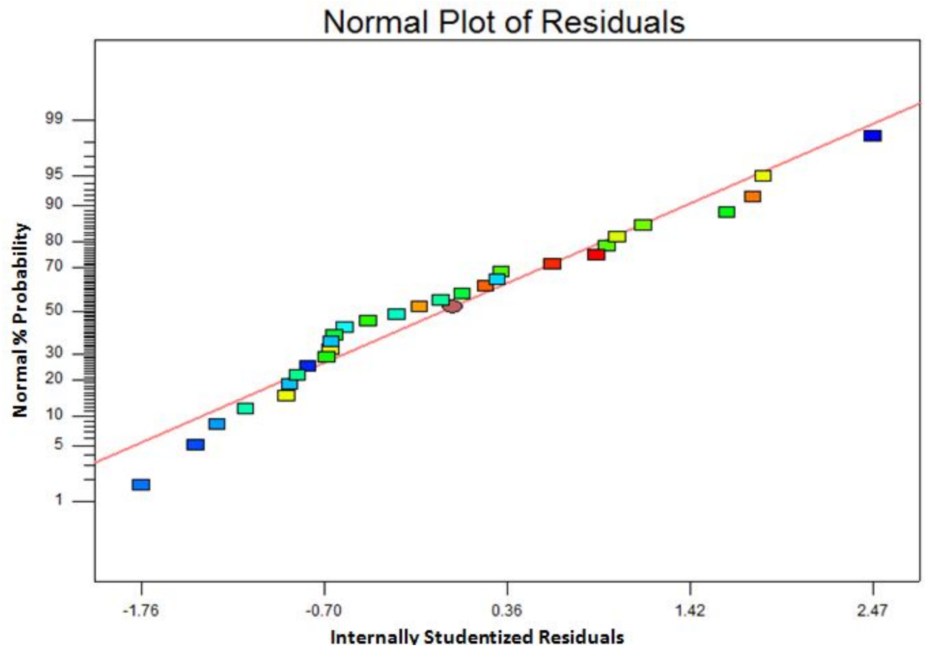

(c) Normal plot of residuals for hardness

Figure 7. normal plot of residuals for impact toughness

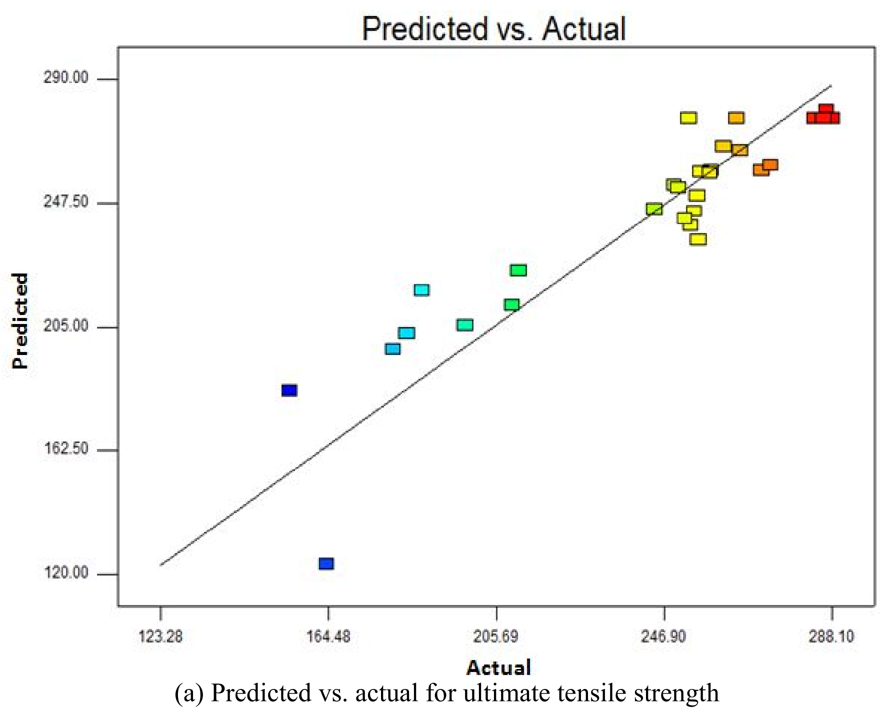

(a) Predicted vs. actual for ultimate tensile strength

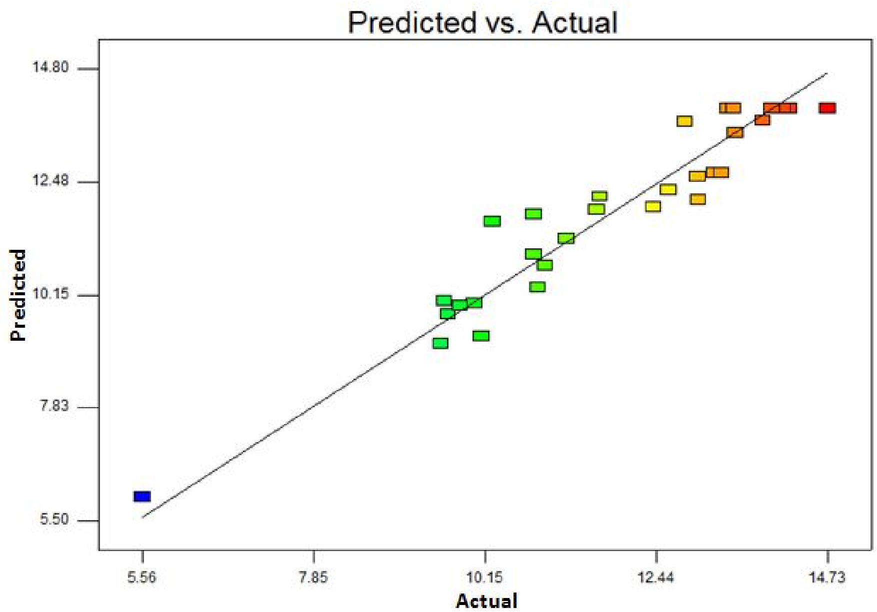

(b) Predicted vs. actual for impact toughness

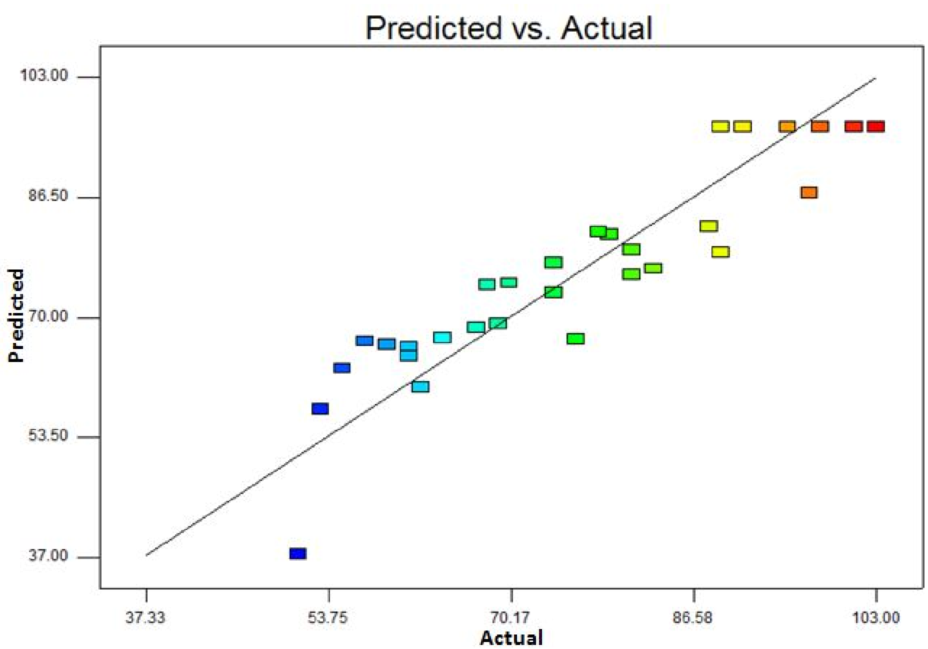

(c) Predicted vs. actual for hardness

Figure 8. Predicted vs. actual

4.3 3D response surface plots for ultimate tensile strength

The response surfaces shown in Figure 9 depict the effect of parameters on ultimate tensile strength. The Figure shows the relationship between two parameters at the center value of the other two parameters. Figure 9(a) shows the effect of tool pin profile and rotational speed. It is clear from the plot that simple cylindrical pin profile produces maximum ultimate tensile strength; whereas, it is minimum for simple tapered pin profile. Figure 9(b) describes the effect of tool pin profile and welding speed. The graph indicates that simple cylindrical tool gives the maximum ultimate tensile strength; however, ultimate tensile strength decreases with the increase in welding speed. Figure 9(c) presents the effect of tool pin profile and tool tilt angle. It can be seen that the ultimate tensile strength is maximum for simple cylindrical tool pin profile; whereas, the effect of tilt angle is nearly constant. The effect of rotational speed and welding speed on ultimate tensile strength has been provided in Figure 9(d). The ultimate tensile strength is maximum at the lower values of rotational speed and welding speed. As the rotational speed and welding speed increases the ultimate tensile strength decreases. Figure 9(e) depicts the effect of rotational speed and tool tilt angle. It is clear that ultimate tensile strength increases with the increase in rotational speed and tilt angle up to maximum value and then decreases with the increase of these two parameters. The effect of welding speed and tool tilt angle on ultimate tensile strength has been presented in Figure 9(f). It can be seen that with the increase in welding speed, ultimate tensile strength decreases; whereas, with the increase in tilt angle the ultimate tensile strength increases up to maximum value and then decreases with increase in tilt angle.

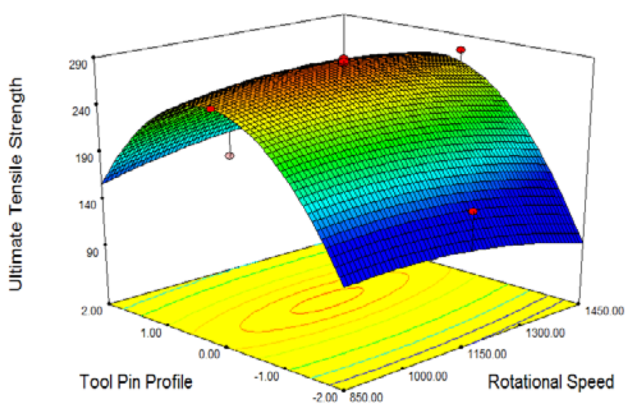

(a) 3D surface UTS vs. tool pin profile and rotational speed

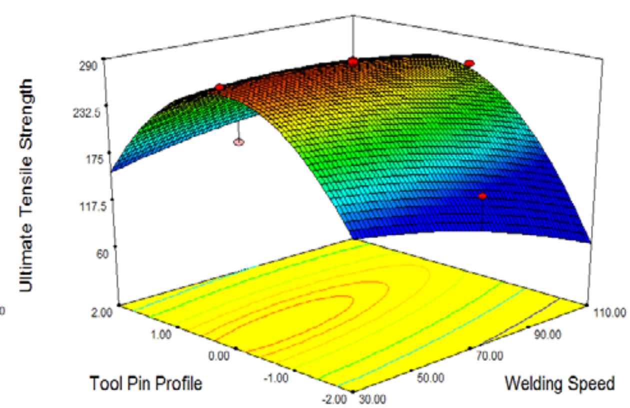

(b) 3D surface UTS vs. tool pin profile and welding speed

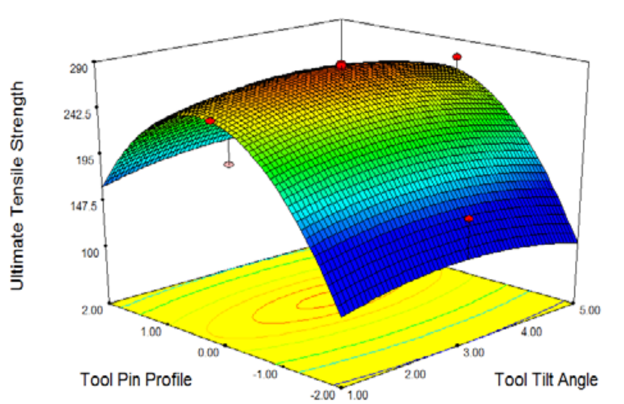

(c) 3D surface UTS vs. tool pin profile and tool tilt angle

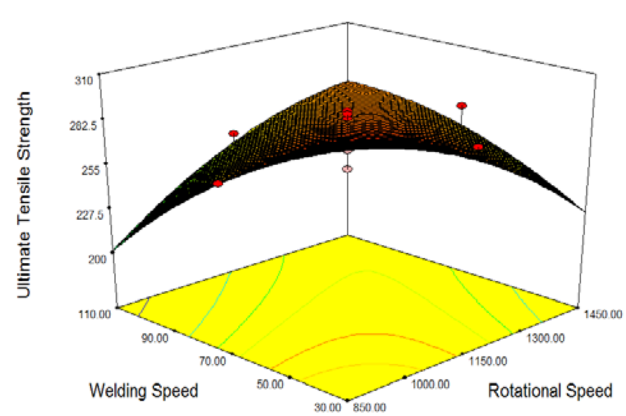

(d) 3D surface UTS vs. rotational speed and welding speed

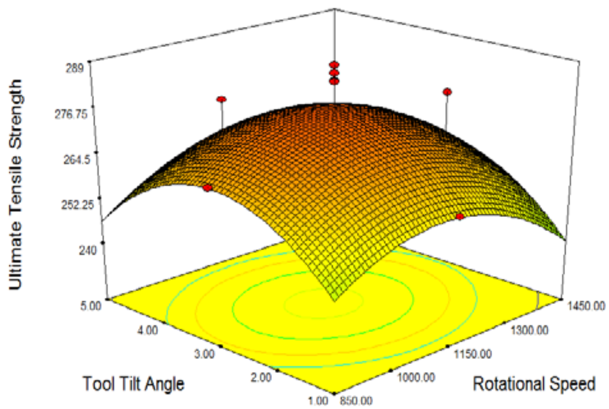

(e) 3D surface UTS vs. rotational speed and tool tilt angle

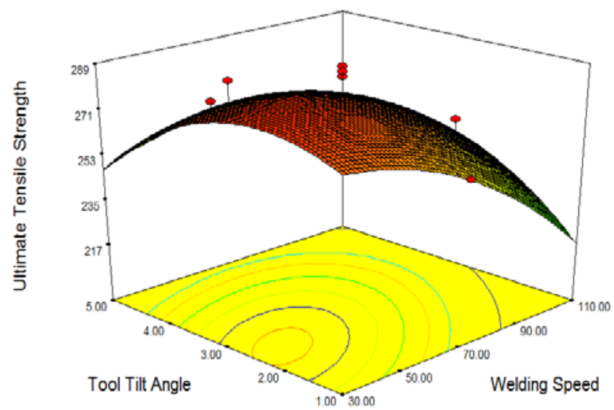

(f) 3D surface UTS vs. welding speed and tool tilt angle

Figure 9. Effect of parameters on UTS

4.4 3D response surface plots for impact toughness

The response surface plots in Figures 10 describe the effect of input parameters on impact toughness. Figure 10(a) demonstrates the effect of tool pin profile and rotational speed on impact toughness. It is clear that simple cylindrical pin profile produces weld with maximum impact toughness and it increases with the increase in rotational speed up to maximum and then decreases. Impact toughness, on the other hand, is minimum for simple tapered pin profile. Figure 10(b) reflects the effect of tool pin profile and welding speed. The Figure indicates that the effect of welding speed on impact toughness is nearly constant while simple cylindrical tool gives the maximum impact toughness. The effect of tool pin profile and tool tilt angle has been described in Figure 10(c). It is evident that the impact toughness is maximum for simple cylindrical tool pin profile, whereas tilt angle has no effect on impact toughness. Figure 10(d) presents the effect of rotational speed and welding speed on impact toughness. The Figure indicates that impact toughness increases with the increase in rotational speed and welding speed up to maximum and then decreases. The effect of rotational speed and tool tilt angle has been demonstrated in Figure 10(e). It is clear from the Figure that impact toughness increases with the increase in rotational speed up to maximum value and then decreases while impact toughness increases with the increase in tool tilt angle. Figure 10(f) shows the effect of welding speed and tool tilt angle on impact toughness. It is observed that impact toughness increases with the increase in welding speed and tilt angle up to maximum value and then decreases with the increase in these two parameters.

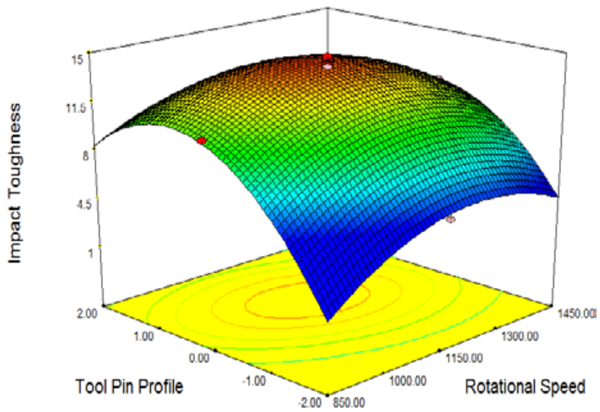

(a) 3D surface impact toughness vs. tool pin profile and rotational speed

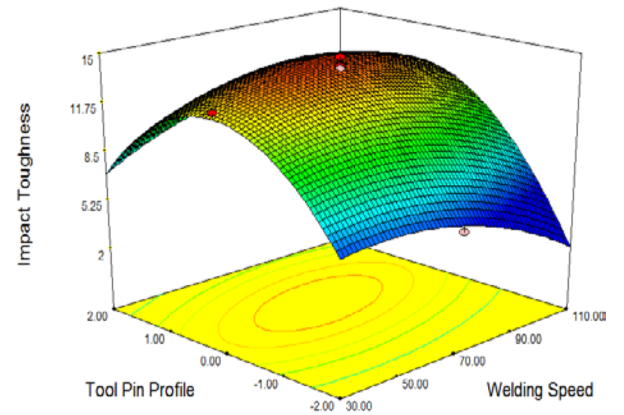

(b) 3D surface impact toughness vs. tool pin profile and welding speed

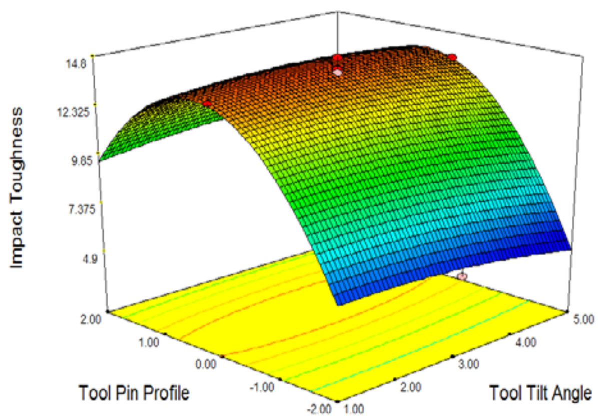

(c) 3D surface impact toughness vs. tool pin profile and tool tilt angle

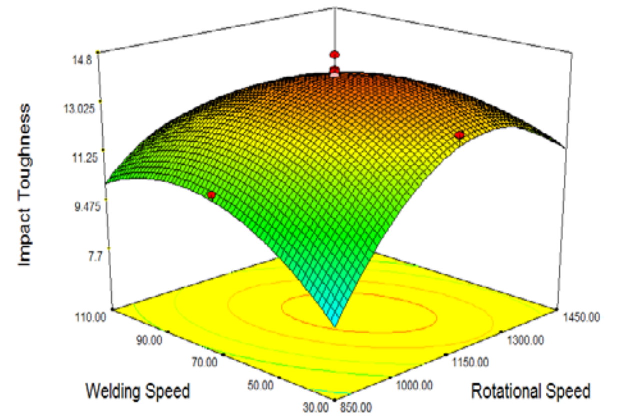

(d) 3D surface impact toughness vs. rotational speed and welding speed

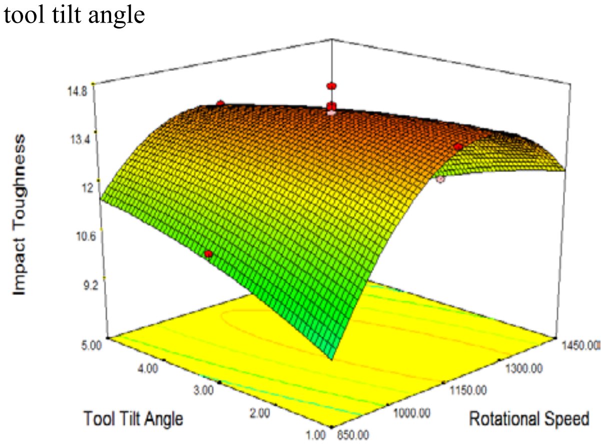

(e) 3D surface impact toughness vs. rotational speed and tool tilt angle

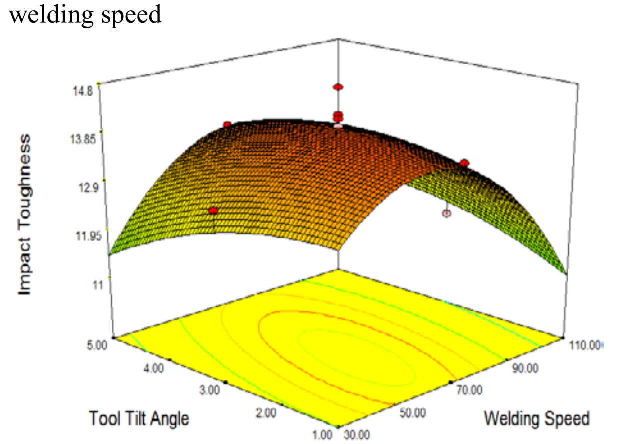

(f) 3D surface impact toughness vs. welding speed and tool tilt angle

Figure 10. Effect of parameters on impact toughness

4.5 3D response surface plots for hardness

The 3D response surface plots shown in Figures 11 present the effect of input parameters on weld hardness. Figure 11(a) represents the effect of tool pin profile and rotational speed. It is clear from the plot that simple cylindrical pin profile produces maximum hardness and it increases up to maximum value with the increase in rotational speed and then decreases. Figure 11(b) describes the effect of tool pin profile and welding speed. The Figure indicates that simple cylindrical tool gives the maximum hardness, however it increases up to maximum value with the increase in welding speed and then decreases. Figure 11(c) depicts the effect of tool pin profile and tool tilt angle. It is clear that the hardness is maximum for simple cylindrical tool pin profile, whereas it increases up to maximum value with the increase in tool tilt angle and then decreases. The effect of rotational speed and welding speed on hardness has been shown in Figure 11(d). It can be seen that hardness increases with the increase in rotational speed and welding speed up to maximum and then decreases. Figure 11(e) reflects the effect of rotational speed and tool tilt angle. It is clear from the Figure that hardness increases with the increase in rotational speed and tilt angle up to maximum value and then decreases with the increase of these two parameters. Figure 11(f) demonstrates the effect of welding speed and tool tilt angle on hardness. It is obsrved that hardness increases with the increase in welding speed and tilt angle up to maximum value and then decreases with the increase in these two parameters.

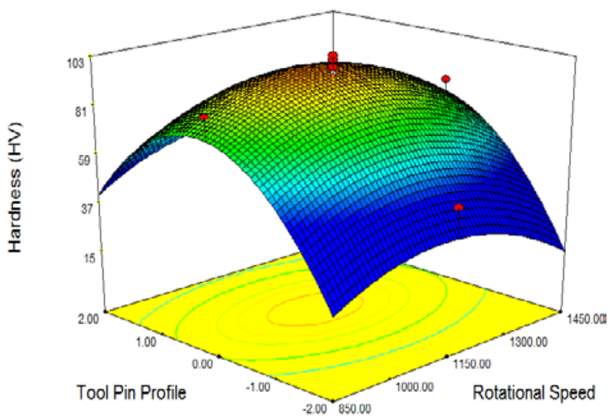

(a) 3D surface hardness vs. tool pin profile and rotational speed

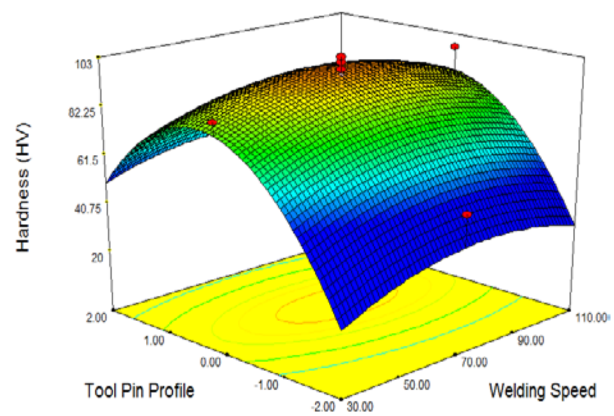

(b) 3D surface hardness vs. tool pin profile and welding speed

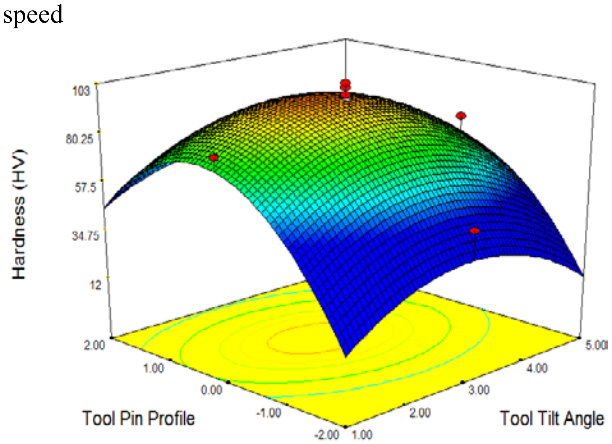

(c) 3D surface hardness vs. tool pin profile and tool tilt angle

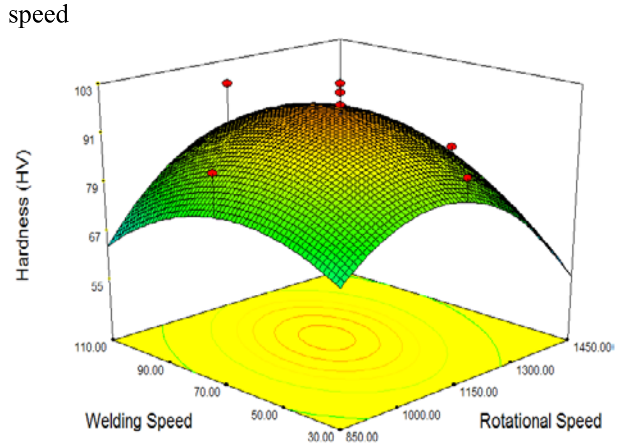

(d) 3D surface hardness vs. rotational speed and welding speed

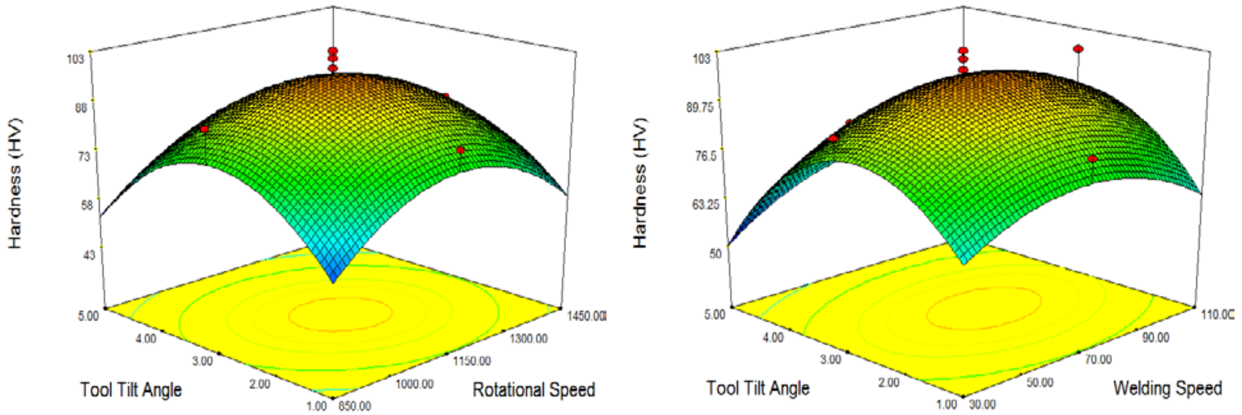

(e) 3D surface hardness vs. rotational speed and tool tilt angle

(f) 3D surface hardness vs. welding speed and tool tilt angle

Figure 11. Effect of parameters on hardness

4.6 Optimum FSW parameters values

The optimum friction stir welding parameters to achieve maximum tensile strength, impact toughness and hardness are shown in Table 8. It is evident from the Table that the highest ultimate tensile strength is achieved at rotational speed of 1150 rpm, welding speed of 70 mm/min, tool tilt angle of 3° and with simple cylindrical pin profile. Interestingly the highest, impact toughness, and hardness values were achieved at the same FSW parameters. These results are in close agreement with the previous work of İpekoğlu et.al. [21] who identified that the hardness is directly affects tensile strength.

Table 8: Optimum FSW parameters values against output responses

Input parameters	
Rotational Speed (rpm)	1150
Welding Speed (mm/min)	70
Tilt Angle	3°
Pin Profile	Simple Cylindrical
Output responses	
UTS (MPa)	288.10
Impact toughness (J)	14.73
Hardness (HV)	103

5. Confirmation test

Three confirmation tests were carried out in order to validate the regression models. The values on which the confirmation tests were performed were within the designed space. However, the confirmation tests were performed on values different from central composit design matrix. The experimental and predicted values of the confirmation tests are presented in Table 9. The error between experimental and predicted values is within 95% confindence interval which varifies that the model is adequate and both the predicted and expermental values are in good agreement with each other. Therefore, it can be concluded that the developed models are applicable for all values within the designed space.

Table 9: Confirmation test results

Experiment	Input parameters				Output responses	Experimental				Predicted	% Error
	Rotational Speed (rpm)	Welding Speed (mm/min)	Tilt Angle	Pin Profile		1st reading	2nd reading	3rd reading	Average		
1	1050	80	2.5	SC	**UTS (MPa)**	267.98	268.92	270.12	269.01	266.00	1.13
					Impact toughness (J)	10.38	10.98	10.38	10.58	11.13	4.94
					Hardness (HV)	87.00	92.00	88.00	89.00	93.00	4.30
2	1280	55	3.2	TT	**UTS (MPa)**	224.05	225.52	225.46	225.01	227.00	0.88
					Impact toughness (J)	14.66	14.61	15.02	14.76	14.23	3.72
					Hardness (HV)	69.00	73.00	71.00	71.00	69.00	2.90
3	1100	75	3.8	CT	**UTS (MPa)**	252.00	253.35	253.65	253.00	256.00	1.17
					Impact toughness (J)	11.45	11.02	11.89	11.45	12.05	4.97
					Hardness (HV)	88.00	85.00	88.00	87.00	83.00	4.81

6. Conclusions

Aluminum alloy 6061-T6 has been joined by FSW. The mechanical properties including ultimate tensile strength, hardness, and impact toughness were investigated using RSM with central composite design. Empirical relations were developed to predict the mechanical properties of the weld. Three confirmation tests were also performed which confirmed that the empirical relations are accurate within 95% confidence level. The following conclusion can be drawn from this investigation:

1) RSM with central composite design was successfuly used to develop a mathematical model for predicting mechanical properties including ultimate tensile strength, impact toughness, and hardness of FS welded AA 6061-T6 joints.

2) The optimum conditions of process parameters, tool pin profile, rotational speed, welding speed, and tool tilt angle, by using developed mathematical model helped to achieve 92% ultimate tensile strength, 87% impact toughness, and 95% hardness of the parent material.

3) The tool pin profile has a significant influence on the mechanical properties of the FS Weld joints. It was observed that simple cylindrical tool pin profile produced joints with miximum mechanical properties.

4) The rotational speed has been identified as more significant parameter than welding speed for ultimate tensile strength and impact toughness, whereas; for hardness welding speed has been identified as more significant parameter than rotational speed.

5) The ultimate tensile strength of the friction stir weld decreases with the increase in rotational speed and welding speed. Impact toughness and hardness, on the other hand, increased up to maximum with the increase in rotational speed and welding speed and then decreases.

6) At rotational speed of 1150 rpm, welding speed of 70 mm/min, tool tilt angle of 3^o and with simple cylindrical pin profile, the highest ultimate tensile strength, impact toughness, and hardness were achieved.

The research findings and developed mathematical models can be successfully used by the practitioners to predict the mechanical strength of AA6061-T6 before welding.

7. References

1. Ericsson M, Sandström R (2003) Influence of welding speed on the fatigue of friction stir welds, and comparison with MIG and TIG. *International Journal of Fatigue 25*(12): 1379-1387
2. Taban E, Kaluc E (2007) Comparison between microstructure characteristics and joint performance of 5086-H32 aluminium alloy welded by MIG, TIG and friction stir welding processes. *Kovove Materialy 45*(5): 241-248
3. Çam G, Koçak M (1998) Progress in joining of advanced materials. *International Materials Reviews 43*(1): 1-44
4. Çam G, Koçak M (1998) Progress in joining of advanced materials: Part 1: Solid state joining, fusion joining, and joining of intermetallics. *Science and Technology of Welding and Joining 3*(3): 105-126
5. Cam G, Koçak M (1998) Progress in joining of advanced materials Part 2: Joining of metal matrix composites and joining of other advanced materials. *Science and Technology of Welding & Joining 3*(4): 159-175

6. Pakdil M, Cam G, Kocak M, Erim S (2011) Microstructural and mechanical characterization of laser beam welded AA6056 Al-alloy. *Materials Science and Engineering: A 528*(24): 7350-7356

7. Çam G, Güçlüer S, Çakan A, Serindag HT (2009) Mechanical properties of friction stir butt-welded Al-5086 H32 plate. *Materialwissenschaft und Werkstofftechnik 40*(8): 638-642

8. Cam G (2011) Friction stir welded structural materials: beyond Al-alloys. *International Materials Reviews 56*(1): 1-48

9. Çam G, Mistikoglu S (2014) Recent developments in friction stir welding of Al-alloys. *Journal of Materials Engineering and Performance 23*(6): 1936-1953

10. Mironov S, Inagaki K, Sato YS, Kokawa H (2015) Effect of welding temperature on microstructure of friction-stir welded aluminum alloy 1050. *Metallurgical and Materials Transactions A*, *46*(2): 783-790.

11. Wu CS, Zhang WB, Lei SHI, Chen, MA (2012) Visualization and simulation of plastic material flow in friction stir welding of 2024 aluminium alloy plates. *Transactions of Nonferrous Metals Society of China 22*(6): 1445-1451

12. Kumar R, Singh K, Pandey S (2012) Process forces and heat input as function of process parameters in AA5083 friction stir welds. *Transactions of Nonferrous Metals Society of China 22*(2): 288-298

13. Saeidi M, Manafi B, Givi MB, Faraji G (2015) Mathematical modeling and optimization of friction stir welding process parameters in AA5083 and AA7075 aluminum alloy joints. *Proceedings of the Institution of Mechanical Engineers, Part B: Journal of Engineering Manufacture.* doi: 10.1177/0954405415573697

14. Bozkurt Y, Salman S, Çam G (2013) Effect of welding parameters on lap shear tensile properties of dissimilar friction stir spot welded AA 5754-H22/2024-T3 joints. *Science and Technology of Welding and Joining 18*(4): 337-345

15. İpekoğlu G, Çam G (2014) Effects of initial temper condition and postweld heat treatment on the properties of dissimilar friction-stir-welded joints between AA7075 and AA6061 aluminum alloys. *Metallurgical and Materials Transactions A 45*(7): 3074-3087

16. Gibson BT, Lammlein DH, Prater TJ, Longhurst WR, Cox CD, Ballun MC, Dharmaraj KJ, Cook GE, Strauss AM (2014). Friction stir welding: process, automation, and control. *Journal of Manufacturing Processes 16*(1): 56-73

17. Moreira PMGP, De Figueiredo MAV, De Castro PMST (2007) Fatigue behaviour of FSW and MIG weldments for two aluminium alloys. *Theoretical and Applied Fracture Mechanics 48*(2): 169-177

18. İpekoğlu G, Erim S, Çam G (2014) Effects of temper condition and post weld heat treatment on the microstructure and mechanical properties of friction stir butt-welded AA7075 Al alloy plates. *The International Journal of Advanced Manufacturing Technology 70*(1-4): 201-213

19. Zhao J, Jiang F, Jian H, Wen K, Jiang L, Chen X (2010) Comparative investigation of tungsten inert gas and friction stir welding characteristics of Al–Mg–Sc alloy plates. *Materials & Design 31*(1): 306-311

20. Lakshminarayanan AK, Balasubramanian V, Elangovan K (2009) Effect of welding processes on tensile properties of AA6061 aluminium alloy joints. *The International Journal of Advanced Manufacturing Technology 40*(3-4): 286-296

21. İpekoğlu G, Erim S, Kıral BG, Çam G (2013) Investigation into the effect of temper condition on friction stir weldability of AA6061 Al-alloy plates. *Kovove Mater 51*(3): 155-163

22. Çam G, İpekoğlu G, Tarık Serindağ H (2014) Effects of use of higher strength interlayer and external cooling on properties of friction stir welded AA6061-T6 joints. *Science and Technology of Welding and Joining 19*(8): 715-720

23. İpekoğlu G, Erim S, Çam G (2014) Investigation into the influence of post-weld heat treatment on the friction stir welded AA6061 Al-alloy plates with different temper conditions. *Metallurgical and Materials Transactions A 45*(2): 864-877

24. İpekoğlu G, Gören Kıral B, Erim S, Çam G (2012) Investigation of the effect of temper condition on friction stir weldability of AA7075 Al-alloy plates. *Mater Technol 46*(6): 627-632

25. Xu W, Liu J, Zhu H, Fu L (2013) Influence of welding parameters and tool pin profile on microstructure and mechanical properties along the thickness in a friction stir welded aluminum alloy. *Materials & Design 47:* 599-606

26. Elangovan K, Balasubramanian V (2008) Influences of tool pin profile and tool shoulder diameter on the formation of friction stir processing zone in AA6061 aluminium alloy. *Materials & design 29*(2): 362-373

27. Palanivel R, Mathews PK, Murugan N, Dinaharan I (2012) Effect of tool rotational speed and pin profile on microstructure and tensile strength of dissimilar friction stir welded AA5083-H111 and AA6351-T6 aluminum alloys. *Materials & Design 40:* 7-16

28. Salari E, Jahazi M, Khodabandeh A, Ghasemi-Nanesa H (2014) Influence of tool geometry and rotational speed on mechanical properties and defect formation in friction stir lap welded 5456 aluminum alloy sheets. *Materials & Design 58:* 381-389

29. Ilangovan M, Boopathy SR, Balasubramanian V (2015) Effect of tool pin profile on microstructure and tensile properties of friction stir welded dissimilar AA6061-AA5086 aluminium alloy joints. *Defence Technology* 11: 174-184

30. Mohanty HK, Mahapatra MM, Kumar P, Biswas P, Mandal NR (2012) Modeling the effects of tool shoulder and probe profile geometries on friction stirred aluminum welds using response surface methodology. *Journal of Marine Science and Application 11*(4): 493-503

31. Bilgin MB, Meran C (2012) The effect of tool rotational and traverse speed on friction stir weldability of AISI 430 ferritic stainless steels. *Materials & Design 33:* 376-383

32. Movahedi M, Kokabi AH, Reihani SS, Najafi H (2012) Effect of tool travel and rotation speeds on weld zone defects and joint strength of aluminium steel lap joints made by friction stir welding. *Science and Technology of welding and joining 17*(2): 162-167

33. Kasman Ş (2013) Multi-response optimization using the Taguchi-based grey relational analysis: a case study for dissimilar friction stir butt welding of AA6082-T6/AA5754-H111. *The International Journal of Advanced Manufacturing Technology 68*(1-4): 795-804

34. Aydin H, Bayram A, Esme U, Kazancoglu Y, Guven O (2010) Application of grey relation analysis (GRA) and Taguchi method for the parametric optimization of friction stir welding (FSW) process. *Mater Tehnol 44(4):* 205-211

35. Jayaraman M, Sivasubramanian R, Balasubramanian V, Lakshminarayanan AK (2009) Optimization of process parameters for friction stir welding of cast aluminium alloy A319 by Taguchi method. *Journal of scientific and industrial research 68*(1): 36

36. Kasman Ş, Kahraman F (2014) Investigations for the effect of parameters on the weld performance of AA 5083-H111 joined by friction stir welding. *Proceedings of the Institution of Mechanical Engineers, Part B: Journal of Engineering Manufacture 228*(8): 937-946

37. Gadakh VS, Kumar A (2013) Friction stir welding window for AA6061-T6 aluminium alloy. *Proceedings of the Institution of Mechanical Engineers, Part B: Journal of Engineering Manufacture.* doi: 10.1177/0954405413510289

38. Ahmadi H, Arab NM, Ghasemi FA (2014) Optimization of process parameters for friction stir lap welding of carbon fibre reinforced thermoplastic composites by Taguchi method. *Journal of Mechanical Science and Technology 28*(1): 279-284

39. Liu HJ, Hou JC, Guo H (2013) Effect of welding speed on microstructure and mechanical properties of self-reacting friction stir welded 6061-T6 aluminum alloy. *Materials & Design 50:* 872-878

40. Li D, Yang X, Cui L, He F, Shen H (2014) *Effect of welding parameters on microstructure and mechanical properties of AA6061-T6 butt welded joints by stationary shoulder friction stir welding.* Materials & Design **64**: 251-260

41. Rajakumar S, Muralidharan C, Balasubramanian V (2011) Predicting tensile strength, hardness and corrosion rate of friction stir welded AA6061-T6 aluminium alloy joints. *Materials & Design 32*(5): 2878-2890

42. Fujii H, Cui L, Maeda M, Nogi K (2006) Effect of tool shape on mechanical properties and microstructure of friction stir welded aluminum alloys. *Materials Science and Engineering: A 419*(1): 25-31

43. Heidarzadeh A, Saeid T, Khodaverdizadeh H, Mahmoudi A, Nazari E (2013) Establishing a mathematical model to predict the tensile strength of friction stir welded pure copper joints. *Metallurgical and Materials Transactions B 44*(1): 175-183

44. Shojaeefard MH, Behnagh RA, Akbari M, Givi MKB, Farhani F (2013) Modelling and Pareto optimization of mechanical properties of friction stir welded AA7075/AA5083 butt joints using neural network and particle swarm algorithm. *Materials & Design*, *44:* 190-198

45. Okuyucu H, Kurt A, Arcaklioglu E (2007) Artificial neural network application to the friction stir welding of aluminum plates. *Materials & design 28*(1): 78-84

46. Hwang YM, Kang ZW, Chiou YC, Hsu HH (2008) Experimental study on temperature distributions within the workpiece during friction stir welding of aluminum alloys. *International Journal of Machine Tools and Manufacture 48*(7): 778-787

47. Roshan, SB, Jooibari MB, Teimouri R, Asgharzadeh-Ahmadi G, Falahati-Naghibi M, Sohrabpoor H (2013) Optimization of friction stir welding process of AA7075 aluminum alloy to achieve desirable mechanical

properties using ANFIS models and simulated annealing algorithm. *The International Journal of Advanced Manufacturing Technology 69*(5-8): 1803-1818

48. Azam M, Jahanzaib M, Wasim A, Hussain S (2015) Surface roughness modeling using RSM for HSLA steel by coated carbide tools. *The International Journal of Advanced Manufacturing Technology 78*(5-8): 1031-1041

49. Elangovan K, Balasubramanian V, Babu S (2009) Predicting tensile strength of friction stir welded AA6061 aluminium alloy joints by a mathematical model. *Materials & Design 30*(1): 188-193

50. Heidarzadeh A, Khodaverdizadeh H, Mahmoudi A, Nazari E (2012) Tensile behavior of friction stir welded AA 6061-T4 aluminum alloy joints. *Materials & Design 37:* 166-173

51. Lotfi AH, Nourouzi S (2014) Predictions of the optimized friction stir welding process parameters for joining AA7075-T6 aluminum alloy using preheating system. *The International Journal of Advanced Manufacturing Technology 73*(9-12): 1717-1737

52. Ilkhichi AR, Soufi R, Hussain G, Barenji RV, Heidarzadeh A (2015) Establishing mathematical models to predict grain size and hardness of the friction stir-welded AA 7020 aluminum alloy joints. *Metallurgical and Materials Transactions B 46*(1): 357-365

53. Montgomery DC (2001) *Design and analysis of experiments 5th edition*, New York: John Wiley and Sons

54. Box GE, Hunter WG, Hunter JS (2005) *Statistics for experimenters II,* Wiley, New York